THE JOURNAL OF BIOLOGICAL CHEMISTRY VOL. 288, NO. 15, pp. 10661–10671, April 12, 2013


# The Ubiquitin-fold Modifier 1 (Ufm1) Cascade of *Caenorhabditis elegans*[S]

Received for publication, February 5, 2013, and in revised form, February 27, 2013 Published, JBC Papers in Press, February 28, 2013, DOI 10.1074/jbc.M113.458000

**Patrick Hertel**[1], **Jens Daniel**[1], **Dirk Stegehake, Hannah Vaupel, Sareetha Kailayangiri, Clio Gruel, Christian Woltersdorf, and Eva Liebau**[2]

*From the Department of Molecular Physiology, Institute for Animal Physiology, University of Muenster, Schlossplatz 8, 48143 Muenster, Germany*

**Background:** The novel ubiquitin-like modifier (UBL) Ufm1 has essential functions in mammalian embryonic development.
**Results:** The Ufm1 cascade in *Caenorhabditis elegans* is required for normal growth and development and is involved in cellular stress response.
Conclusions: The *C. elegans* Ufm1 cascade is an antagonist of the unfolded protein response.
**Significance:** The *C. elegans* Ufm1 cascade offers a unique opportunity to understand the fundamentals underlining this UBL.

**Ufm1 (ubiquitin-fold modifier 1) is the most recently identified member of the ubiquitin-like protein family. We characterized the Ufm1 cascade of the model organism *Caenorhabditis elegans* in terms of function and analyzed interactions of the involved proteins *in vitro* and *in vivo*. Furthermore, we investigated the phenotypes of the deletion mutants *uba5*(ok3364) (activating enzyme of Ufm1) and *ufc1*(tm4888) (conjugating enzyme of Ufm1). The viable deletion mutants showed a decrease in reproduction, development, life span, and a reduced survival under heavy metal stress. However, an increased survival rate under pathogenic, oxidative, heat, and endoplasmic reticulum stress was observed. We propose that the Ufm1 cascade negatively regulates the IRE1-mediated unfolded protein response.**

Many essential cellular processes require changes in protein activity, stability, and intracellular localization. The high variability of the proteome is guaranteed by specific posttranslational protein modifications, including small polypeptides such as ubiquitin (Ub)[3] and ubiquitin-like proteins (UBLs). The process of marking a protein by Ub and UBLs is catalyzed by a sequential reaction of multiple enzymes, forming an isopeptide bond between the modifier and the target protein. The cascade consists of E1 (activating), E2 (conjugating), and E3 (ligating) enzymes. Ub and UBLs have been shown to be involved in an extraordinary large variety of cellular processes such as cell cycle, cell differentiation, DNA repair, gene transcription, protein quality control, signal transduction, endocytosis, and receptor trafficking (reviewed in Refs. 1–3).

In recent years, various human diseases have been associated with a defective regulation of substrate modifications by the UBL pathways, illustrating the tremendous significance for the organism (4, 5). Ufm1 (ubiquitin-fold modifier 1) is one of the newest and less characterized members of the UBL family that is conserved in metazoa and plants. The 9.1-kDa protein possesses an ubiquitin-like $\beta$-grasp fold, although it hardly shares any sequence identity (16%) with Ub (6).

Similar to Ub and many UBLs, Ufm1 is synthesized as a proform and cleaved at the C terminus to expose a conserved Gly residue. This maturation step is mediated by two Ufm1 specific cysteine proteases UfSP1 and UfSP2 (7). Thereafter, Ufm1 is covalently conjugated to target proteins through an enzymatic cascade, consisting of Uba5 (ubiquitin-like modifier activating enzyme 5, E1), Ufc1 (Ufm1 conjugating enzyme 1, E2), and Ufl1 (Ufm1-specific ligase 1, E3, also known as KIAA0776, RCAD, NLBP, and Maxer) (Fig. 1). The resulting conjugates are cleaved by the same specific proteases (UfSP1/2) used for Ufm1 maturation, implying the reversibility of the Ufm1 cascade (6, 8). Ufbp1 (Ufm1 binding protein 1 with a PCI domain; C20orf116) represents the first identified target protein of the Ufm1 cascade and is highly conserved in multicellular organisms (8, 9). A function of Ufbp1 has not been described so far. In addition to a hydrophobic N terminus that acts as a signal anchor in the outer ER membrane, a C-terminal PCI (proteasome-COP9-initiation factor) domain was identified (10, 11).

So far, the physiological function of the Ufm1 cascade is poorly understood. Tatsumi *et al.* (8) demonstrated that *uba5*$^{-/-}$ knock-out mice died *in utero* due to severe anemia that was associated with defective differentiation of megakaryocytes and erythrocytes. Their results demonstrated the essential role of the Ufm1 system in erythroid differentiation.

Other studies clearly demonstrate a close association between the Ufm1 cascade and the endoplasmic reticulum (ER) (9, 12–14). The ER is responsible for synthesis and folding of secretory and membrane proteins. Correctly folded proteins exit the ER and are transported through the Golgi apparatus to

[S] This article contains supplemental Tables 1–6 and Figs. 1 and 2.
[1] Both authors contributed equally to this work. This work was submitted to the University of Münster to fulfill the requirements of a part of the Ph.D. thesis.
[2] To whom correspondence should be addressed: Dept. of Molecular Physiology, Inst. for Animal Physiology, University of Muenster, Schlossplatz 8, 48143 Muenster, Germany. Tel.: 49-251-83-21710; Fax: 49-251-83-21766; E-mail: liebaue@uni-muenster.de.
[3] The abbreviations used are: Ub, ubiquitin; UPR, unfolded protein response; ER, endoplasmic reticulum; Ni-NTA, nickel-nitrilotriacetic acid; DCLA, differential cytolocalization assay; mUfm1, mature Ufm1; MTLS, membrane tether localization signal.

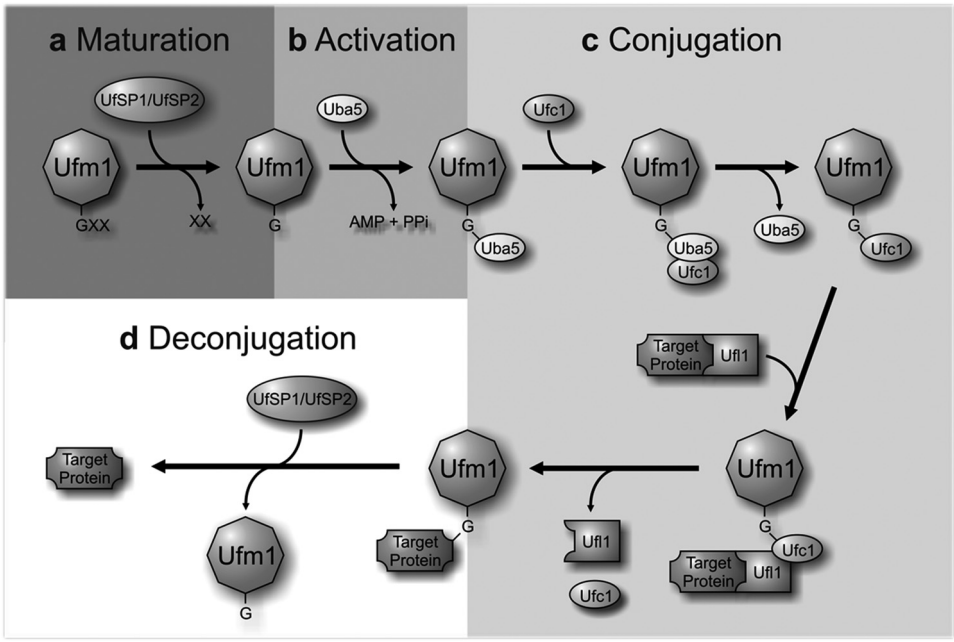


FIGURE 1. **The Ufm1 conjugation pathway.** *a*, maturation. The Ufm1-specific proteases UfSP1 and UfSP2 process the C-terminal extension of the Ufm1 precursor, exposing a conserved glycine residue. *b*, activation. The mature Ufm1 is activated by Uba5 (E1) in an ATP-dependent manner, forming a high-energy thioester bond. *c*, conjugation. The activated Ufm1 is then transferred to Ufc1 (E2) in a similar thioester linkage. The E3 enzyme Ufl1 enables the transfer of Ufm1 to the target protein, thereby forming an isopeptide bond between Ufm1 and its substrate. *d*, deconjugation. The proteases UfSP1 and UfSP2 also mediate the deconjugation of Ufm1.

their corresponding destinations (15). Misfolded proteins remain in the ER, and their accumulation can lead to ER stress. Several adjustments, which are collectively referred to as the unfolded protein response (UPR), exist to cope with ER stress. To coordinate the ER stress response, the three membrane-bound UPR signal transducers IRE1 (inositol-requiring protein-1), PERK (protein kinase RNA-like endoplasmic reticulum kinase) and the bZIP family transcription factor ATF6 (activating transcription factor 6) are used (15, 16).

Ufm1 is up-regulated in pathological conditions that are associated with activation of the ER stress response such as type II diabetes and ischemic heart injury (9, 12). Recently, Zhang *et al.* (17) were able to demonstrate that Ufm1 is a potential target of Xbp-1 (x-box binding protein 1), a crucial IRE1-dependent transcription factor in UPR.

In the present study, the Ufm1 cascade of the model organism *Caenorhabditis elegans* was characterized in terms of function and composition. Stage- and tissue-specific expression patterns were analyzed, and protein/protein interactions were confirmed *in vitro* and *in vivo*. We provide evidence that the Ufm1 cascade is involved in the stress response toward various stressors and takes a regulatory function in the ER stress response in *C. elegans.* A potential role in cadmium detoxification is discussed.

## EXPERIMENTAL PROCEDURES

*Plasmid Constructs and Oligonucleotides*—Plasmid constructs and oligonucleotides were used for thioester formation and pulldown assays (supplemental Table 1), expression pattern analysis (supplemental Table 2), differential cytolocalization assay (DCLA) (supplemental Table 3), and yeast two-hybrid assays (supplemental Table 4).

*Worm Strains*—Worms strains were cultured and maintained as described previously (18). Worm populations were synchronized by alkaline hypochlorite lysis (19). The following strains were obtained from the *Caenorhabditis* Genetics Center at the University of Minnesota: wild-type N2 Bristol, *rCes F38A5.1*::*GFP*+*pCeh361*;*dpy-5 (e907)I*, *zcIs4 V*[*hsp-4*::*GFP*]; *upr-1 (zc6)X*, *pha-1(e2123)III*, and *uba5(ok3364)I. ufc1*(tm4888)*III* were obtained from the National BioResource Project. *uba5(ok3364)I* and *ufc1*(tm4888)*III* were outcrossed six times to the wild-type N2 Bristol prior to use.

*Transgenic C. elegans*—Germ line transformation was performed by coinjection of vector constructs (80 $\mu$g/ml) with the plasmid pRF4, encoding the dominant marker gene *rol-6* (50 $\mu$g/ml). pBX containing the dominant marker gene *pha-1* (20) was used for microinjecting *pha-1* animals. Selection of transgenic animals of the *pha-1*/pBX system is based on the temperature-sensitive embryonic lethal mutation *pha-1*. After microinjection, the animals were transferred to 25 °C. Only transformed progeny survive and can be easily maintained by cultivation at 25 °C. For visualization, animals were immobilized in 2.5 mM levamisole and analyzed using a laser-scanning microscope TCS SP2 (Leica).

*Recombinant Expression*—For the generation of tagged recombinant proteins, the vectors pJC40 (His tag), pGEX-4T2 (GST tag), and pASK-IBA3plus (streptomycin tag) were used. Protein expression was performed overnight (18 h) using 0.5 mM isopropyl 1-thio-$\beta$-D-galactopyranoside or by autoinduction (21). Cell lysis was performed via sonification. The tagged proteins were purified using specific matrixes (Ni-NTA-agaraose (Qiagen), glutathione agarose (Sigma-Aldrich), or Strep-Tactin-Sepharose (IBA)) following the manufacturer's instructions.

*In Vitro Thioester Formation Assay*—The thioester formation assay was performed as described in Ref. 6. The following recombinant proteins were produced in *Escherichia coli* and were N-terminally tagged with GST: GST-Uba5, GST-Uba5$^{C250S}$, GST-Ufm1, and GST-Ufm1$^{G83A}$. The GST-tagged proteins were purified using glutathione-agarose (Sigma-Aldrich). Following elution of the proteins using 10 mM GSH (reduced glutathione) in 10 mM Tris/HCl, pH 8.0, the eluted proteins were dialyzed against the thioester formation buffer (50 mM BisTris (pH 6.5), 100 mM NaCl, 10 mM $MgCl_2$, and 0.1 mM DTT). Most thioester formation reactions contained reaction buffer with 5 $\mu$g GST-Ufm1 or GST-Ufm1$^{G83A}$ and some of the following: 5 mM ATP, 10 mM $MgCl_2$, 100 mM DTT, 100 mM GSH, or 15 $\mu$g or 30 $\mu$g of GST-Uba5 or GST-Uba5$^{C260S}$. Reactions were incubated for 1 h at 25 °C and stopped by the addition of SDS-containing loading buffer either lacking reducing agent or containing 100 mM DTT, followed by a 10-min incubation at 37 °C, SDS-PAGE, and Coomassie Blue staining and immunodetection.

*Pulldown Assays*—Pulldown assays were performed according to Ref. 22. To test the interaction between Uba5 and Ufc1, 30 $\mu$g of streptomycin-tagged purified Uba5 was loaded onto Strep-Tactin-Sepharose (IBA) and incubated for 2 h at 4 °C. After extensive washing with 100 mM Tris/HCl, pH 8.0, 150 mM NaCl, 1 mM EDTA, 200 $\mu$l of His-tagged Ufc1 *E. coli* lysate was applied and incubated again for 2 h. Following extensive washing, the protein complex was eluted with 100 mM Tris/HCl, pH 8.0, 150 mM NaCl, 1 mM EDTA, and 2.5 mM D-desthiobiotin, followed by immunodetection. The pulldown assay was also performed by loading His-tagged Ufc1 onto Ni-NTA-agarose, followed by extensive washing in 50 mM Tris/HCl (pH 8.0), 500 mM NaCl, 10% glycerol, 20 mM imidazole; 0.1% Triton and incubated with *E. coli* lysate containing GST-tagged Uba5. Following prolonged washing, the protein complex was eluted using 50 mM Tris/HCl (pH 8.0), 500 mM NaCl, 200 mM imidazole, and 0.1% Triton X-100.

*Yeast Two-hybrid*—A Gal4p-based two-hybrid system (23) was used in this study. The yeast strain SMY3 (24) was transfected and used for two-hybrid screens as described (25). All proteins of interest were cloned both in the AD vector pGAD.GH and the BD vector pGBT9.BS. Selection for interactions were performed on plates containing selection medium that lacked leucine, tryptophan, and histidine (SC-Leu-Trp-His) and was supplemented with 5 or 15 mM 3-amino-1,2,4-aminotriazole. As a weak positive control of an interaction, we used CBL1 (calcineurin B-like) and CIPK23 (CBL-interactin protein-kinase). Alternatively, as a strong positive control of an interaction, we used AKT1 (protein kinase B) and CIPK (26). Yeast strain and positive controls were kind gifts from J. Kudla (University of Münster, Münster, Germany).

*DCLA*—The DCLA is a novel *in vivo* interaction assay for *C. elegans* that allows the investigation of cytoplasmatic protein-protein interactions by visualization of the relocalization of GFP-tagged prey by a membrane-bound bait. The method takes advantage of the vector pPD122.36, which carries both an N-terminal GFP signal and a C-terminal membrane anchor (membrane tether localization signal (MTLS)). Coding regions that are fused with GFP or MTLS were inserted downstream of the myo-3 promoter (27).

*Localization Studies*—Localization studies were performed via microinjection of the vector pPD95.77 containing GFP constructs with native gene promoters (2–3 kb).

*Phenotyping*—To determine the adult life span, 10 larvae were transferred on 10 NGM plates, respectively. The plates were sealed with a palmitic acid ring. After the beginning of egg laying (day = 0), the worms were transferred to new NGM-plates every second day until the end of egg deposition. The survival was measured each day via touch response. Bagging or crawling off of the agar was censored from the statistical analysis. Survial curves were inferred with the Kaplan-Meier method.

To determine postembryonic development, staged adult hermaphrodites were transferred on NGM plates for egg deposition. After 3–4 h, the adult worms were removed. The development was scored after 24, 48, and 72 h.

Reproduction rate was determined by transferring L4 worms onto NGM plates. Worms were transferred on new plates daily, and offspring were counted. All of the above-mentioned assays were performed in three independent trials with at least 10 worms/plate for each group.

All stress survival assays were performed with staged young adults. They were cultivated on plates with the stressors juglone (0.2 mM), cumene (2 mM), cadmium chloride (3 mg/ml), tunicamycin (40 $\mu$g/ml), or DTT (15 mM). The heat stress assay was performed at 31.5 °C. The survival was scored after 16 h of incubation, with the exception of tunicamycin (9 days). A worm was scored as dead when it did not respond to a mechanical stimulus. Each experiment was performed at least three times with 10 × 10 worms.

*Bacillus thuringiensis Stress Assay*—To investigate the resistance against pathogen stress, crystal-toxins of two nematocidal *B. thuringiensis* strains (B-18247 medium toxicity and B-18679 heavy toxicity) were used. The strain DSM 350, which produces nontoxic Cry-proteins was used as negative control. All strains were generous gifts from H. Schulenburg (University of Kiel). The generation of lysate with Cry-toxins was performed as described (28). 5 $\mu$l of the lysate was circled with a narrow palmitic acid ring.

*RNAi*—RNAi assays were carried out as described (29). The RNAi construct for Kel-8 (V-2M20) was obtained from the RNAi library from the Medical Research Council. As a negative control, the empty RNAi vector L4440 was used. Synchronized L1 larvae were grown on RNAi bacteria until they were young adults. These were then used in cadmium stress tests and carried out in M9 buffer containing 50 $\mu$M cadmium chloride.

*Analysis of hsp4-GFP Expression in uba5(ok3364) Deletion Mutants*—To investigate the involvement of the Ufm1 cascade in the UPR, hsp4-GFP(zcIs4)V were crossed into the *uba5*(ok3364) mutant. GFP-signal was quantified under normal and stress conditions (5 $\mu$g/ml tunicamycin (8 h), 10 mM DTT (16 h), 0.1 mM juglone (16 h), 15 mM methyl viologen/paraquat (16 h), 2.5 mM *t*-butylhydroperoxide (16 h), 34 °C (3 h), 200 mM NaCl (16 h)). For visualization, animals were immobilized in 2.5 mM levamisole and analyzed using a fluorescence microscope (Olympus IX50).

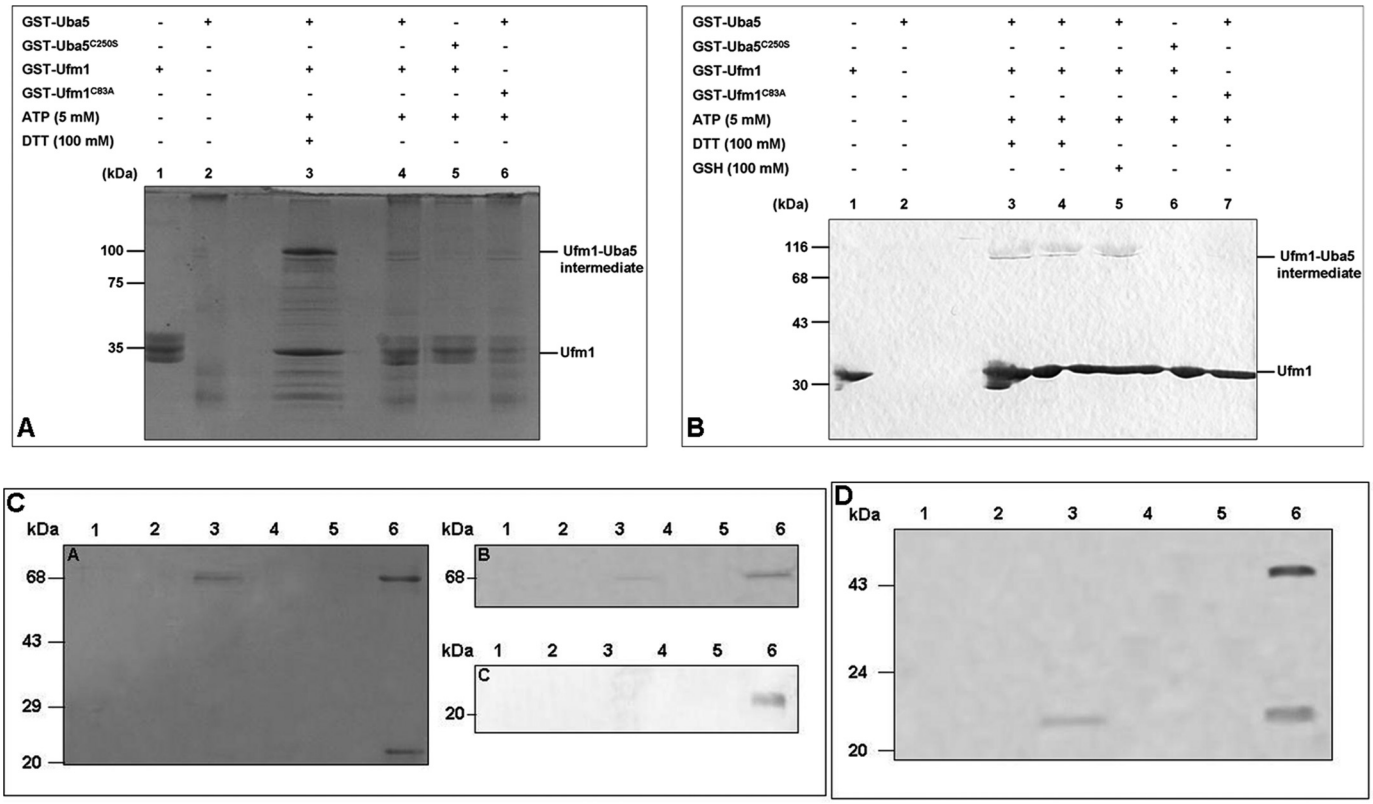


FIGURE 2. **Uba5 activates Ufm1 in *C. elegans*.** *A*, GST-tagged Ufm1 (GST-Ufm1) was incubated for 1 h at 25 °C with the following components: GST-Uba5 (*lanes 2–4* and *6*), GST-Uba5$^{C250S}$ (*lane 5*), and ATP (*lanes 3–6*). One reaction was incubated with the reducing agent DTT (*lane 3*). Samples were subjected to SDS-PAGE and stained with colloidal Coomassie G-250. The Ufm1-Uba5 intermediate was observed in *lane 3* under reducing conditions as indicated on the *right*. *B*, for immunoblotting, a similar *in vitro* activation assay was performed. GST-Ufm1 was incubated with the respective components: GST-Uba5 (*lanes 2–5* and *7*), GST-Uba5$^{C250S}$ (*lane 6*), ATP (*lanes 3–7*), DTT (*lanes 3* and *4*), and GSH (*lane 5*). The samples were subjected to SDS-PAGE and analyzed by immunoblotting with anti-Ufm1 antibody. The bands corresponding to Ufm1 and Ufm1-Uba5 intermediate (*lanes 3–5*) are indicated on the *right*. The interaction of Uba5 with Ufc1 in *C. elegans* was analyzed by His-tagged pulldown assay (*C*) and by streptomycin-tagged pulldown assay (*D*). His-tagged Ufc1 was immobilized on a Ni-NTA-agarose and incubated with GST-Uba5 cell lysate. After extensive washing, the complex was eluted from the matrix (*lane 6*). Loading of His-Ufc1 (*lane 1*) followed by washing (*lane 2*), loading of GST-Uba5 (*lane 3*) followed by washing (*lane 4*), elution of GST-Uba5 (control, *lane 5*), elution of Uba5-Ufc1 intermediate (*lane 6*). After Coomassie staining (*left*), the proteins were identified via immunoblotting using anti-GST antibody (*upper panel*) and anti-His antibody (*lower panel*). The interaction was also analyzed by streptomycin-tagged pulldown assay. Streptomycin-tagged Uba5 (*Strep-Uba5*) was immobilized on Strep-Tactin-Sepharose and incubated with His-Ufc1 cell lysate. After extensive washing, the complex was eluted from the matrix (*lane 6*). Loading of streptomycin-tagged Uba5 (*lane 1*) was followed by washing (*lane 2*), loading of His-Ufc1 (*lane 3*) followed by washing (*lane 4*), elution of His-Ufc1 (control, *lane 5*), and elution of the Uba5-Ufc1 intermediate (*lane 6*).

## RESULTS

*Identification of the Ufm1 Cascade in C. elegans*—Using WormBase, the following components have been identified in *C. elegans*: ZK652.3 (Ufm1), T03F1.1 (Uba5, E1), C40H1.6 (Ufc1, E2), C06G3.9 (Ufl1, E3), target protein ZK1236.7 (Ufbp1), F38A5.1 (UfSP2), Y113G7B.16 (CDK5Rap3), and another potential interacting partner W02G9.2 (Kel-8).

*Uba5 Activates Ufm1 in Vitro*—We analyzed the Ufm1 activation by Uba5 in *C. elegans* with a thioester formation assay (6). Therefore, GST-tagged Uba5 and mature Ufm1 (mUfm1, exposed C-terminal Gly$^{83}$ residue) were recombinantly expressed in *E. coli*, purified, and incubated in the presence of ATP, $MgCl_2$, and DTT (Fig. 2*A*). Samples were subjected to SDS-PAGE under reducing and nonreducing conditions. A protein band with a size of ~100 kDa, corresponding to the calculated molecular mass of the intermediate complex GST-Ufm1-Uba5-GST, was exclusively observed under reducing conditions (Fig. 2*A*, *lane 3*). This intermediate was not visible when the reducing agent DTT was missing (Fig. 2*A*, *lane 4*). Furthermore, no intermediate was formed with the mutant proteins Uba5$^{C250S}$ (active site Cys$^{250}$ mutant) and Ufm1$^{G83A}$ (C-terminal Gly$^{83}$ residue replaced with alanine) under reducing and nonreducing conditions (Fig. 2*A*, *lanes 5* and *6*).

To confirm the formation of the intermediate complex (GST-Ufm1-Uba5-GST), the corresponding 100-kDa protein band was excised and analyzed by mass spectrometry. All components were identified (data not shown).

Subsequently, immunoblotting analysis of the thioester assay was carried out using the self-generated polyclonal *C. elegans* anti-Ufm1 antibody (Fig. 2*B*). Direct addition of DTT (*lane 3*) or GSH (*lane 5*) to the incubation mixture or the addition of DTT to the SDS sample buffer (*lane 4*) led to the formation of the intermediate (100 kDa, Fig. 2*B*). No complex formation was detected when using the two mutant proteins Uba5$^{C250S}$ and Ufm1$^{G83A}$ (Fig. 2*B*, *lanes 6* and *7*). In summary, the *in vitro* analysis revealed that the ATP-dependent intermediate formation between the cysteine at position 250 of Uba5 and the C-terminal Gly$^{83}$ residue of Ufm1 exclusively takes place under reducing conditions.

Moreover, a distinct Uba5 protein band was only detected, following the addition of DTT in the washing buffers used for

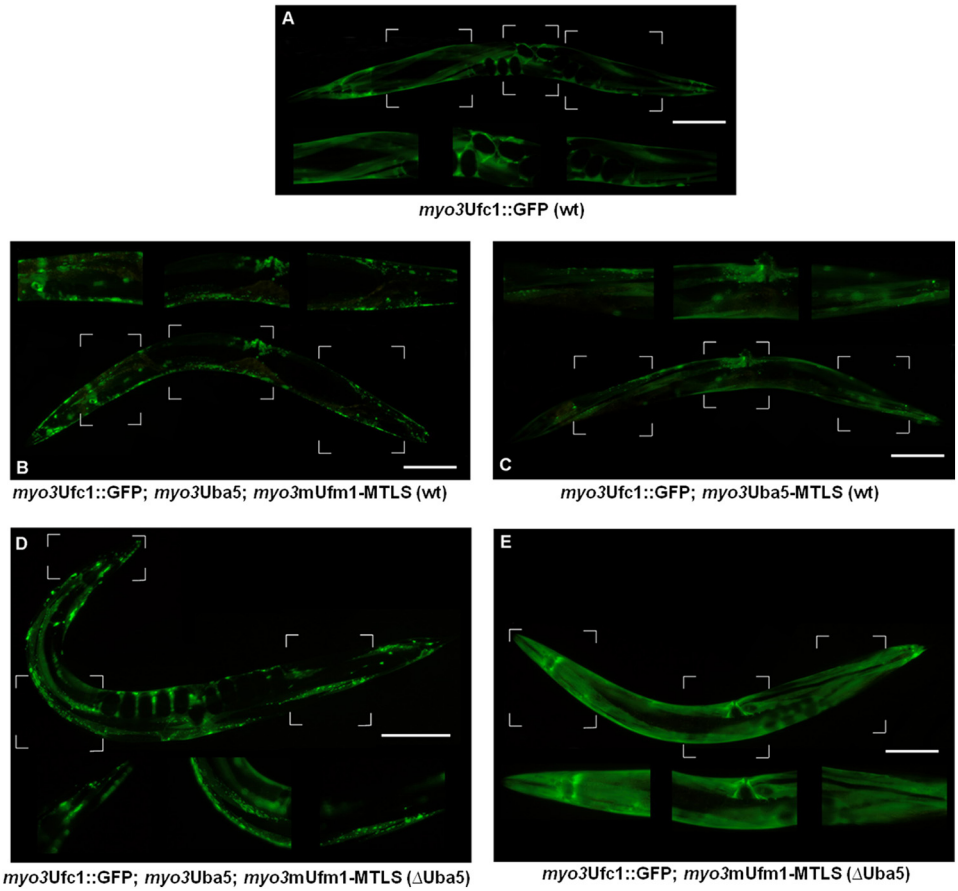


FIGURE 3. **Ufm1, Uba5, and Ufc1 interact *in vivo* in *C. elegans*.** *A*, due to the *myo3* promoter Ufc1::GFP is expressed in body wall muscles. Diffuse cytosolic expression is observed. *B*, Ufc1::GFP is co-expressed with Uba5 and mUfm1-MTLS. Membrane-bound localization is observed, indicating strong interaction. *C*, Ufc1::GFP is co-expressed with Uba5-MTLS. Partial membrane-bound localization is observed. *D*, DCLA of *B* was carried out in the *uba5*(ok3364) deletion mutant. Membrane-bound localization is observed. *E*, DCLA of *C* was carried out in the *uba5*(ok3364) mutant. No interaction occurred in the absence of Uba5. *Scale bar*, 100 $\mu$m.

purification. The absence of DTT led to degradation or aggregation products (data not shown). Therefore, *C. elegans* Uba5 exhibits a different redox sensitivity compared with the human homolog, where the opposite effect of DTT for the intermediate formation was observed (6, 30).

*Uba5 Interacts with Ufc1 in Vitro*—The second step of the Ufm1 cascade includes the Ufm1 transfer from Uba5 to Ufc1. This interaction was analyzed by pulldown assay using Ni-NTA-agarose (Fig. 2*C*). No binding of the GST-Uba5 fusion protein to the Ni-NTA-agarose was observed in the controls (Fig. 2*C*, *A panel*). A 70-kDa (GST-Uba5) and 24-kDa (His-Ufc1) protein band were detected in the elution fraction by Coomassie-stained SDS-PAGE (Fig. 2*C*, *A panel*, *lane 6*). The Western blot analysis (Fig. 2*C*, *B* and *C panels*, *lane 6*) confirmed the *in vitro* interaction of Uba5 and Ufc1. Additionally, a streptomycin tag pulldown assay was performed using streptomycin-tagged Uba5 and His-tagged Ufc1. The obtained results also confirmed the interaction between Uba5 and Ufc1 *in vitro* (Fig. 2*D*).

*Ufm1 Interacts with Ufc1 in Vivo*—The DCLA is a novel method to visualize protein-protein interactions in *C. elegans* as relocalization of GFP-tagged prey proteins by membrane-bound MTLS bait proteins (27). Our interaction studies focused on the core elements of the Ufm1 cascade: Ufm1, Uba5, and Ufc1. The generated GFP-tagged or MTLS-carrying proteins were under the control of the endogenous myosin promoter *myo3*, which shows a strong expression pattern in the muscle cells of *C. elegans*. All constructs were microinjected into the gonads of *C. elegans*. Because cytosolic protein expression of the prey-protein is a basic requirement for the DCLA, we firstly determined the cytosolic localization of *myo3*Ufc1-GFP in muscle cells (Fig. 3*A*).

The activation of mUfm1 by Uba5 takes place under ATP consumption and forms a thioester linkage, which is afterward transferred to Ufc1, forming the Ufm1-Ufc1 complex (6, 31). We investigated the interaction between Ufm1 and Ufc1 by using the constructs *myo3*mUfm1-MTLS and *myo3*Ufc1::GFP in WT worms. Because we could not detect any expression of Uba5 in muscle cells (Fig. 4*D*), *myo3*Uba5 was additionally microinjected. We observed membrane-bound *myo3*Ufc1::GFP localization, indicating an interaction with *myo3*mUfm1-MTLS (Fig. 3*B*).

To clarify the dependence of the mUfm1/Ufc1 interaction on Uba5, we used the deletion mutant *uba5*(ok3364) as a genetic background. *myo3*mUfm1-MTLS and *myo3*Ufc1::GFP were microinjected into the deletion mutant, and the observed cytosolic GFP expression pattern (Fig. 3 E) resembled that of *myo3*Ufc1::GFP (Fig. 3*A*). This indicated no interaction between mUfm1/Ufc1 in the absence of Uba5.

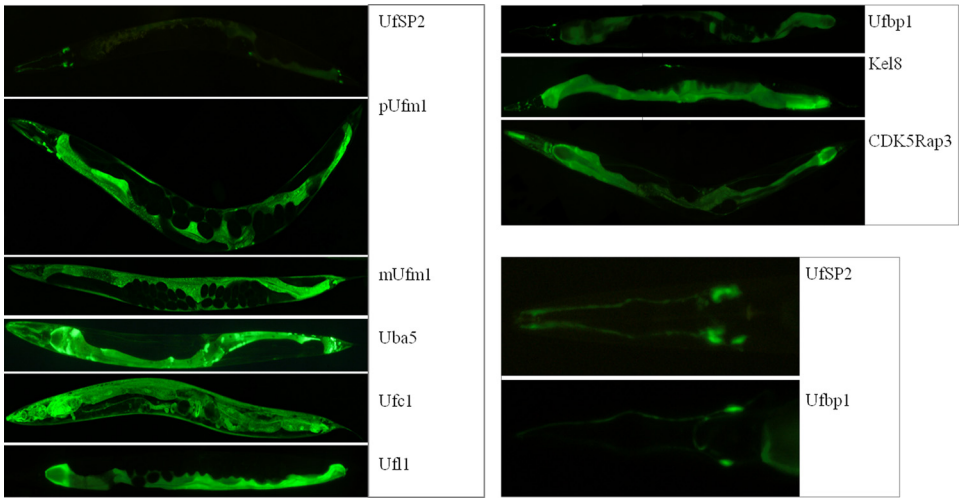


FIGURE 4. **Expression pattern of the Ufm1 system and putative interacting partners in *C. elegans*.** The expression was set under the control of the respective promoter sequences (size, 2–3 kb) of the corresponding genes. Because no stage-specific expression was observed, only adult worms are displayed. The Ufm1 cascade and its potential binding partners are mainly expressed in the intestine. Neuronal expression could be observed in UfSP2, pUfm1, Ufbp1, Kel-8, and CDK5Rap3. The expression of UfSP2 and Ufbp1 in head neurons (possibly amphid neurons) is shown on the *right*.

This result was confirmed by the addition of *myo3*Uba5 to the injection mixture (Fig. 3*D*). Here, we observed a membrane-bound GFP localization in the *uba5*(ok3364) deletion mutant.

Furthermore, we analyzed the interaction of Uba5/Ufc1 *in vivo* bausing the constructs *myo3*Uba5-MTLS and *myo3*Ufc1::GFP (Fig. 3*C*). A partial membrane-bound GFP-localization was determined, indicating weak interaction between Uba5/Ufc1 *in vivo*.

In summary, we showed that mUfm1 interacts *in vivo* with Ufc1 in an Uba5-dependent manner. Furthermore, we observed a weak interaction between Uba5 and Ufc1 *in vivo*.

*Yeast Two-hybrid Analysis*—The yeast two-hybrid system was additionally used for interaction analyses of the Ufm1 cascade and potential interaction partners in *C. elegans*. Therefore, the coding sequences of UfSP2, Ufm1, Uba5, Ufc1, Ufl1, Ufbp1, and the potential interaction partner Y113G7b.16 (*C. elegans* homolog to CDK5Rap3 (32, 33)) and Kel-8 (34) were successfully cloned and co-transfected into yeast cells. All interactions determined are collectively summarized in Table 1. Strong interactions were observed between UfSP2/Ufm1, UfSP2/Kel-8, Ufm1/Ufl1, Ufm1/Ufbp1, Ufl1/Ufbp1, Ufl1/CDK5Rap3, and Ufbp1/CDK5Rap3 and weak interaction between Uba5/Ufc1 was determined. No interactions of Kel-8/Ufc1, CDK5Rap3/Ufc1, and CDK5Rap3/Ufm1 were observed in the yeast two-hybrid studies (supplemental Fig. 1).

*Localization of the Ufm1 Cascade and Potential Binding Partners in C. elegans*—To identify the tissue and temporal localization of the Ufm1 cascade components as well as their potential partners, GFP reporter gene analyses were performed. The expression was set under the control of the putative promoter sequences (size, 2–3 kb) of the corresponding genes.

Except for [*rCes F38A5.1*::*GFP*+*pCeh361*], which was provided by the *Caenorhabditis* Genetics Center, all transgenic lines were generated by us. The promoter analysis of Uba5 and Ufc1 (3 kb promoter + gene) and of Ufl1, Ufbp1, Kel-8, and CDK5Rap3 (2-kb promoter) were fused C-terminal with GFP. As the protease UfSP2 processes Ufm1 at the C terminus (7), GFP was fused N-terminal to proUfm1 and mUfm1. Because the GFP localization exhibits no stage-specific expression, only adult worms are displayed in Fig. 4.

**TABLE 1**

**Summary of all protein/protein interactions analyzed in this study**

A detailed description of the interaction assays used is given under "Experimental Procedures."

| Ufm1 cascade and interacting proteins | Interaction assays |
|---|---|
| Ufm1/UfSP2 | Yeast two-hybrid |
| Ufm1/Uba5 | Thioester formation assay |
| Ufm1/Ufc1 | DCLA |
| Ufm1/Ufl1 | Yeast two-hybrid |
| Uba5/Ufc1 | Yeast two-hybrid/DCLA/pulldown assay |
| Ufbp1/Ufm1 | Yeast two-hybrid |
| Ufbp1/Ufl1 | Yeast two-hybrid |
| CDK5Rap3/Ufl1 | Yeast two-hybrid |
| CdDK5Rap3/Ufbp1 | Yeast two-hybrid |
| Kel-8/UfSP2 | Yeast two-hybrid |

mUfm1, Uba5, and Ufc1::GFP worms were also analyzed under oxidative, ER, and heat stress. We could not observe any differences in the GFP signals (data not shown).

In summary, the localization studies identified a partially strong and ubiquitous expression of the Ufm1 cascade and its potential binding partners mainly in the intestine. Several proteins also showed a neuronal expression. Here, UfSP2 was expressed almost exclusively in several head and tail neurons. In contrast to the localization pattern described in WormBase, its intestinal expression was very limited. On a subcellular level, an increased perinuclear localization of UfSP2 was observed, pointing to an ER-associated expression. The target protein Ufbp1 showed a distinct neuronal expression, possibly in the same amphid neurons as UfSP2 (Fig. 4, *right panel*).

*The Deletion Mutants uba5(ok3364) and ufc1(tm4888)*—The mutant *uba5*(ok3364), generated by the Gene Knock-out Consortium, is characterized by a 827-bp DNA deletion, which leads to the loss of the active site ($Cys^{250}$) of the protein. Because Uba5 is the only Ufm1-activating enzyme, a knock-out of this protein results in the complete inactivation of the Ufm1 cascade. In contrast to mouse studies performed by Ref. 8, the *C. elegans* deletion mutant *uba5*(ok3364) is viable and allows loss-of-function studies throughout the complete life cycle.

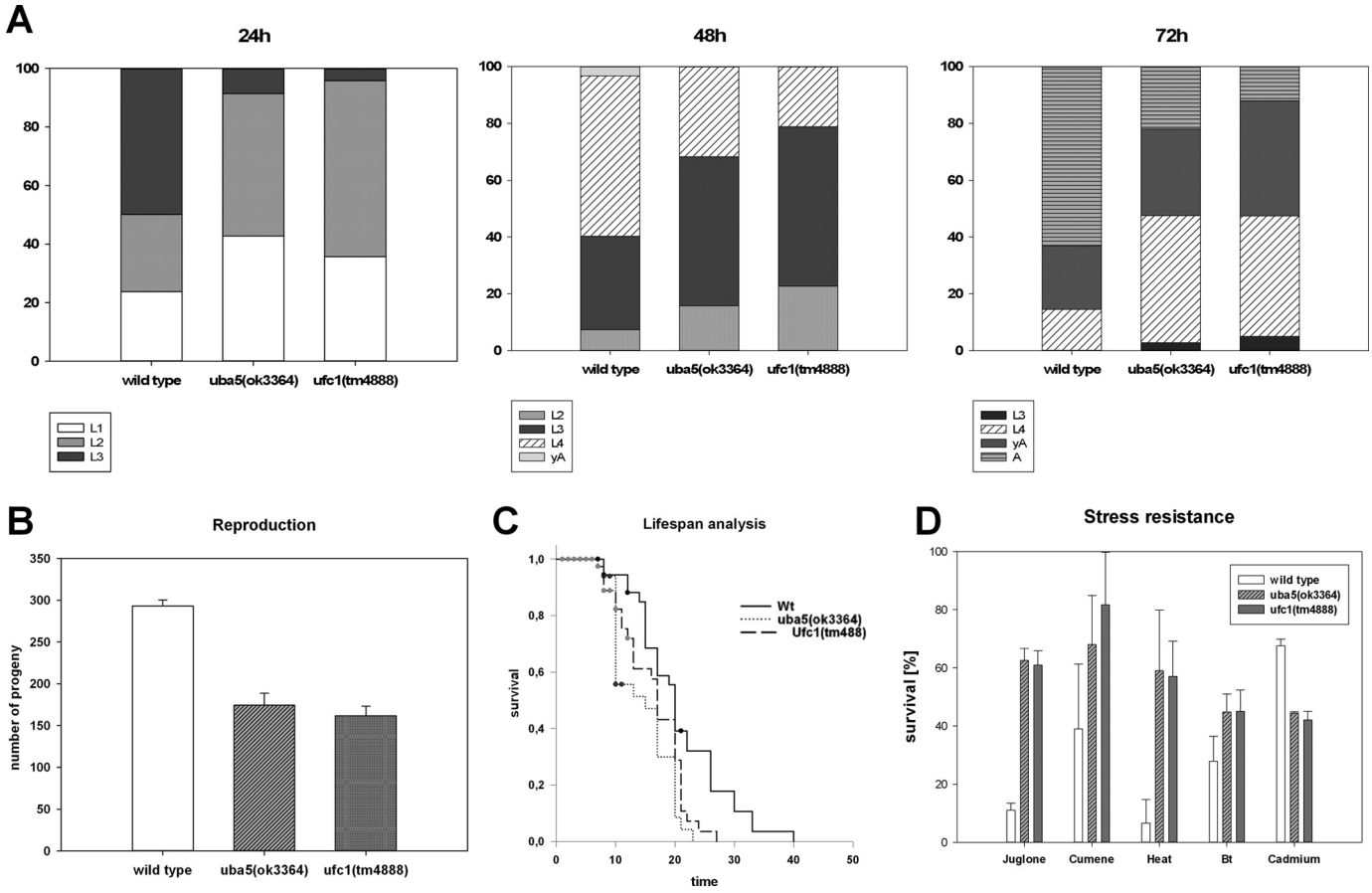


FIGURE 5. **Phenotyping of the *uba5*(ok3364) and *ufc1*(tm4888) deletion mutants.** *A*, the development of larvae was analyzed 28, 48, and 72 h after hatching. The deletion mutants *uba5*(ok3364) and *ufc1*(tm4888) showed a similar delayed development, compared with the wild type. *B*, *uba5*(ok3364) and *ufc1*(tm4888) laid in average 174 and 161 eggs, respectively. Compared with the wild type (average, 293 eggs), the reproduction rate of both mutants was highly significant reduced ($p < 0.0001$) but did not significantly differ toward each other. *C*, the adult lifespan of the deletion mutants (average of 14.6 days for *uba5*(ok3364) and 16.4 days for *ufc1*(tm4888)) was significantly reduced ($p < 0.05$) compared with the wild type (average of 20.8 days) but did not differ when compared to each other. *D*, the survival of the *uba5*(ok3364) and *ufc1*(tm4888) was significantly increased under oxidative, heat, and *B. thuringiensis* stress ($p \leq 0.0001$ for juglone, $p \leq 0.001$ for cumene, $p \leq 0.01$ for heat, and $p < 0.05$ for *B. thuringiensis*). The survival of both mutants under cadmium stress was highly significantly reduced ($p < 0.001$). The mutants did not differ significantly.

The mutant *ufc1*(tm4888), generated by the National BioResource Project, possesses a 413-bp deletion starting in the second intron and covering two of four exons. If Ufc1 is the only E2 enzyme of the Ufm1 cascade, the loss of function should create a similar phenotype to the *uba5* deletion. The usage of two deletion mutants of the Ufm1 cascade also creates a stronger link between the observed phenotype and the function of the cascade.

*Morphology and Reproduction Rate*—Both mutants were viable under standard conditions and did not display any obvious morphological or behavioral phenotypes.

The average reproduction rates of *uba5*(ok3364) and *ufc1*(tm4888) were analyzed under normal culturing conditions (Fig. 5*B*). Although wild type worms laid an average of 293 eggs, the deletion mutants *uba5*(ok3364) and *ufc1*(tm4888) laid an average of 174 and 162 eggs, respectively. Although the mutants did not show a significant difference between each other, the difference toward the wild type worms was highly significant ($p \geq 0.001$).

*Larval Development*—For a comparative determination of the temporal larval development, synchronous *C. elegans* cultures of the deletion mutants *uba5*(ok3364) and *ufc1*(tm4888) were cultivated under standard conditions. After 24, 48, and 72 h, the larval development was documented (Fig. 5*A*). Both deletion mutants showed a similar delayed development compared with the WT worms. After 48 h, >50% of the WT worms had reached the L4 stage, and few were already young adults. In contrast, most mutants were still at the L3 stage, and none had reached the adult stage. Although no difference between the deletion mutants could be observed, both displayed a highly significant developmental delay compared with the WT controls ($p \geq 0.001$). After 72 h, most of the WT worms had started to lay eggs, whereas the deletion mutants were still in the L4 or young adult stage ($p \geq 0.01$, no significant difference between the mutant strains).

*Adult Life Span*—The adult life span of the deletion mutants was analyzed under standard conditions (Fig. 5*C*). Although WT worms lived ~21 days, the deletion mutants *uba5*(ok3364) and *ufc1*(tm4888) lived 15 or 16 days, respectively ($p \geq 0.01$, no significant difference between the mutant strains).

*Stress Resistance*—To further investigate the involvement of the Ufm1 cascade in stress response, survival stress assays were carried out with both deletion mutants (*uba5*(ok3364) and *ufc1*(tm4888)) (Fig. 5*D*). The survival rate was determined in

the presence of the pathogenic *B. thuringiensis* strain BT-18247, metal stress (cadmium, 3.0 mg/ml, 16 h, 20 °C), oxidative stress (juglone, 0.2 mM, cumene 2 mM, 16 h, 20 °C), and heat stress (31.5 °C, 16-h + 2-h recovery at 20 °C).

Direct comparison between *uba5*(ok3364) and *ufc1*(tm4888) mutants showed no significant difference under all stress conditions analyzed. However, both mutant strains demonstrated a significant enhanced survival rate toward pathogen, heat, and oxidative stress ($p \leq 0.0001$ for juglone, $p \leq 0.001$ for cumene, $p \leq 0.01$ for heat, and $p < 0.05$ for *B. thuringiensis*). Interestingly, the resistance against cadmium was significantly reduced ($p \leq 0.001$).

Taken together, loss of function of the Ufm1 cascade leads to a reduced reproduction rate, a reduced life span, and a developmental delay of ~6 h. Although an enhanced stress tolerance can be observed under pathogenic, heat, and oxidative stress, the survival in the presence of cadmium was greatly reduced.

*ER Stress and the Ufm1 Cascade*—Various studies demonstrated associations of the Ufm1 cascade with the ER (8, 9, 12, 13, 17). To investigate the involvement of the Ufm1 cascade in UPR regulation, we used the ER stress reporter strain *hsp4*-GFP(zcIs4)V (*Caenorhabditis* Genetics Center, strain SJ6). Here, the promoter region of the *C. elegans* ortholog of BiP/GRP78 (*hsp4*) is fused to GFP and integrated into the worm genome (35). Under ER stress conditions, the UPR signal transducer IRE1 and the subsequent transcription factor Xbp-1 regulate the Hsp4-GFP expression in *C. elegans* (35). Thus, GFP intensity indicates ER stress.

First, we analyzed whether knockdown of components of the Ufm1 cascade (*ufm1* and *uba5*) causes ER stress *per se*. However, no increased *hsp4*-GFP fluorescence was observed compared with the control (data not shown). We next examined the influence of the Ufm1 cascade knockdown on the Hsp4-expression under stress. Therefore, the ER stressor tunicamycin, which inhibits glycosylation in the ER, was used. The *in vivo* studies determined an elevated Hsp4 expression under stress due to the knockdown of Ufm1 and Uba5 (data not shown).

To further investigate the role of the Ufm-1 cascade in UPR, we crossed the *uba5*(ok3364) deletion mutant with the ER stress reporter line *hsp4*-GFP(zcIs4)V. Under standard conditions, we could observe a weak increase in GFP signal (Fig. 6). In the next step, we applied various stressors that range from ER (tunicamycin, DTT), oxidative (juglone, *t*-BOOH, paraquat), osmo (NaCl), and UV, up to heat stress. Under all of the conditions analyzed, the *uba5* deletion led to a consistent increase of the Hsp4 expression (Fig. 6). However, under DTT stress, we observed high variations in the GFP signals that were not present in the other stress experiments. Therefore, the DTT stress results are presented proportionally (Fig. 6).

Finally, the survival rate of the *uba5*(ok3364)::*hsp4*-GFP strain was investigated under ER stress (tunicamycin, DTT). According to the Student's *t* test calculations, the *uba5* deletion led to an increased survival rate ($p \leq 0.0001$) under ER stress (Fig. 6).

Taken together, the loss of function of the Ufm1 cascade led to an increased IRE1 activity under various stress conditions. Interestingly, we also observed an increased survival rate under ER stress.

## DISCUSSION

The role of the Ufm1 cascade in multicellular organisms remains largely elusive. The present study has identified the enzymes involved in the activation and conjugation of Ufm1 in *C. elegans.* We could demonstrate the E1 activity of Uba5 and show the interactions of the Ufm1 components with each other and with the target protein Ufbp1 and CDK5Rap3. Furthermore, we show the involvement of the Ufm1 cascade in the resistance toward different environmental stressors and provide evidence of a regulatory function in the ER stress response in *C. elegans*.

The Ufm1 cascade and the two target proteins are mainly expressed in the intestine and in various neurons. Because the *C. elegans* intestine combines the functions of liver and kidney (36), the observed expression might reflect the localization pattern observed in mammals, where an increased expression in the liver, kidney, and brain was reported (6–8).

In contrast to most animals, *C. elegans* possesses only one Ufm1-specific protease, the longer UfSP2. Although the activity of murine UfSP1 was shown (14), it seems to be non-functional in other mammals, indicating that UfSP2 is the essential and conserved protease for the Ufm1 system.

UfSP2 mediates the maturation of the Ufm1 precursor and is capable of releasing Ufm1 from Ufm1-conjugated cellular proteins (7). A T868C transition in exon 8 of UfSP2, substituting $Tyr^{290}$ with histidine, results in Beukes hip dysplasia in humans (37). Recently, the up-regulation of the Ufm1 cascade during osteogenic differentiation was shown, pointing to a possible involvement of the Ufm1 pathway in Beukes hip dysplasia.[4]

*C. elegans* UfSP2 is mainly expressed in chemosensory neurons, localized in the head and tail region. Because UfSP2 shows an extremely low expression in the intestine, an essential role in the maturation of Ufm1 appears improbable. It seems more likely that UfSP2 is a deconjugating enzyme of Ufm1 in neurons. Here, the subcellular localization of UfSP2 indicates an ER association also observed in mammals (14). We propose a deconjugating function of UfSP2 at the ER membrane of chemosensory neurons.

We confirmed Kel-8 as an interacting partner of the Ufm1 system by an *in vitro* interaction with UfSP2. Kel-8, which also shows a neuronal expression pattern, mediates the ubiquitin-dependent degradation of rapsyn and the GLR-1 subunit of the AMPAR glutamate receptor in post-synapses of *C. elegans* (38, 39). It is also involved in cadmium detoxification in association with Bcmo-1 and Mek-1 (40). Although RNAi knockdown of Kel-8 in WT worms mediates a strong decrease of survival under cadmium stress, no effect could be observed in the *uba5*(ok3364) deletion mutant, pointing to a potential involvement of the Ufm1 cascade in the Kel-8 mediated cadmium detoxification (see supplemental Fig. 2).

The CDK5Rap3 of *C. elegans* has not yet been characterized. It is probably associated with CDK5 and therefore

[4] M. Dudek, unpublished observation.

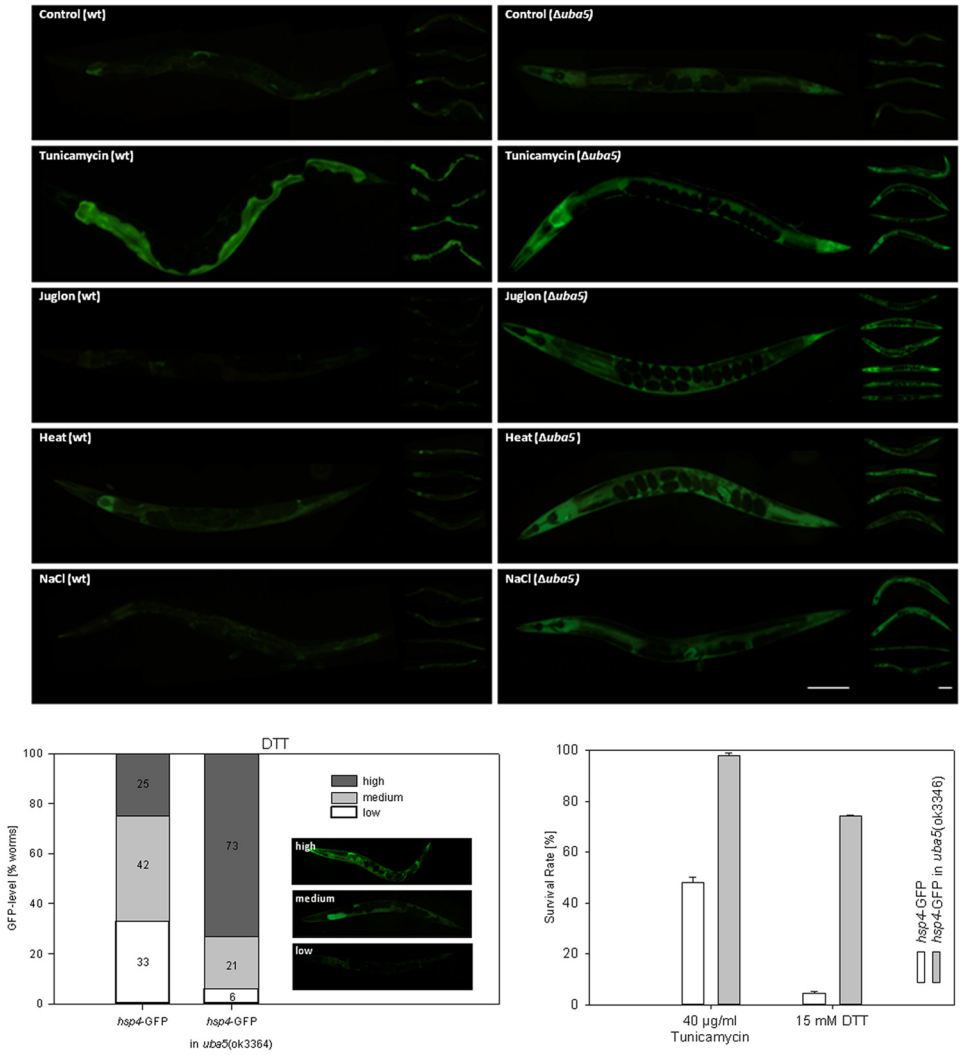


FIGURE 6. **Increased Hsp4 expression in the deletion mutant *uba5*(ok3364) under various stress conditions.** The expression of the reporter gene construct hsp4-GFP was visually examined and analyzed under standard and various stress conditions in the deletion mutant *uba5*(ok3364) and in wild type worms. A consistent increase of the GFP signal could be observed in the deletion mutant under tunicamycin, juglone, heat, and NaCl stress. Since the expression pattern observed under DTT stress was highly variable, a percentage distribution of GFP levels (low, medium, high) is given. The *uba5*(ok3364) worms also displayed a highly significant increased survival under tunicamycin (97.6% compared with 48% in wild type $p < 0.01$) and DTT (74.2% survival compared with 4.6% in wild type, $p > 0.01$) (*right panel*).

involved in the regulation of pronuclear migration and neuronal development.[5]

The deletion of Uba5 or Ufc1 caused a similar and viable phenotype. Although a reduced reproduction rate, a reduced life span and a developmental delay was observed in both mutants, an enhanced stress tolerance toward pathogenic, oxidative, heat, and ER stress was shown. The decreased reproduction rate and developmental delay of the deletion mutants can be explained in terms of rerouting carbohydrate flux from the generation of ATP through glycolysis, to the generation of NADPH and redox equivalents through the pentose phosphate pathway, to counteract cellular stress.

Recent proteomic analysis revealed a changed GAPDH expression pattern in the *uba5*(ok3364) deletion mutant.[6] Therefore, we are currently investigating the role of the Ufm1 cascade in the regulation of GAPDHs because they represent key enzymes in energy metabolism (41).

In our *in vitro* thioester formation assay, we observed that the Ufm1 activation by Uba5 is a redox-sensitive process. In contrast to data described previously (6), the Ufm1 activation in *C. elegans* only occurred under reducing conditions. This might point to a potential regulation of Ufm1 conjugation by the redox status of the cell. A stress-mediated oxidative shift in the cellular redox status might inhibit the Ufm1 conjugation and therefore promote stress response.

The Ufm1 cascade has been linked to ER homeostasis in general and to the IRE1 pathway specifically (17, 42). IRE1 is the

[5] S. N. Williams, K. A. Caldwell, and G. A. Caldwell (2001). Phenotypic Crosstalk Between the LIS-1 and Cdk5 Pathways in C. elegans, presented at the Thirteenth International Worm Meeting, University of California, Los Angeles, June 22–26, 2001.

[6] P. J. Hertel, J. Daniel, D. Stegehake, H. Vaupel, S. Kailayangiri, C. Gruel, C. Woltersdorf, and E. Liebau, unpublished data.

most conserved UPR pathway and, in contrast to humans, regulates all major chaperones and UPR genes in *C. elegans* (42). Accumulation of unfolded or damaged proteins not only occurs under various stress conditions but also in embryonic and larval development. Therefore, the UPR does not only represent a stress response but also a mechanism to retain the cellular homeostasis in general (43). Furthermore, Richardson *et al.* (43) showed a rapid activation of the IRE1 pathway caused by the innate immune response of *C. elegans* toward pathogen stress.

By reporter gene analysis using the BiP homolog Hsp4, we demonstrated an increased IRE1 activity in the absence of the Ufm1 cascade under various stress conditions. Because this increase was also associated with an improved survival rate, the observed stress resistance of the *uba5*(ok3364) deletion mutants could at least be partially linked to the IRE1 activity. Given that the activity of the Ufm1 cascade in *C. elegans* negatively regulates the UPR and other stress responses, the cascade appears to be involved in restoring homeostasis and balancing energy metabolism, therefore promoting growth and reproduction.

Interestingly, the Ufm1 cascade was found to protect against ER stress-mediated apoptosis in secretory cells of mammals (9, 17). Zhang *et al.* (17) showed an important role of the Ufm1 cascade in the ER homeostasis of murine cells. Furthermore, the knock-out of Uba5 in mice led to the apoptosis of erythroid progenitors (8, 44). Both Lemaire *et al.* (9) and Zhang *et al.* (17) concluded that the Ufm1 cascade protects against ER stress and therefore prevents apoptosis. However, in *C. elegans*, where apoptotic events only occur during development of hermaphrodites, the Ufm1 cascade was shown to inhibit UPR. We therefore propose that the apoptotic events that take place in pancreatic beta cells (9) and erythroid progenitors (44) in the absence of Ufm1 conjugation, are not the result of an increased ER stress but of an increased cellular stress response.

We have established *C. elegans* as a suitable model system for the Ufm1 cascade. *C. elegans* offers the possibility to perform *in vivo* protein/protein interaction analysis, loss-of-function analysis of members of the Ufm1 cascade and also promising approaches to further investigate the connection of Ufm1 to the UPR and to stress response homeostasis in general.

Further studies will concentrate on changes observed on transcriptome and proteome level caused by the loss of the Ufm1 cascade.

*Acknowledgments—We highly appreciate the scientific advice of K. Lemaire and F. Schuit. The hard work of students is acknowledged. We thank J. Kudla for helpful discussions concerning yeast two-hybrid assays.*

## REFERENCES


1. van der Veen, A. G., and Ploegh, H. L. (2012) Ubiquitin-like proteins. *Annu. Rev. Biochem.* **81,** 323–357
2. Hochstrasser, M. (2009) Origin and function of ubiquitin-like proteins. *Nature* **458,** 422–429
3. Kirkin, V., and Dikic, I. (2007) Role of ubiquitin- and Ubl-binding proteins in cell signaling. *Curr. Opin. Cell Biol.* **19,** 199–205
4. Bedford, L., Lowe, J., Dick, L. R., Mayer, R. J., and Brownell, J. E. (2011) Ubiquitin-like protein conjugation and the ubiquitin-proteasome system as drug targets. *Nat. Rev. Drug Discov.* **10,** 29–46
5. Kim, K. I., and Baek, S. H. (2009) Small ubiquitin-like modifiers in cellular malignancy and metastasis. *Int. Rev. Cell Mol. Biol* **273,** 265–311
6. Komatsu, M., Chiba, T., Tatsumi, K., Iemura, S., Tanida, I., Okazaki, N., Ueno, T., Kominami, E., Natsume, T., and Tanaka, K. (2004) A novel protein-conjugating system for Ufm1, a ubiquitin-fold modifier. *EMBO J.* **23,** 1977–1986
7. Kang, S. H., Kim, G. R., Seong, M., Baek, S. H., Seol, J. H., Bang, O. S., Ovaa, H., Tatsumi, K., Komatsu, M., Tanaka, K., and Chung, C. H. (2007) Two novel ubiquitin-fold modifier 1 (Ufm1)-specific proteases, UfSP1 and UfSP2. *J. Biol. Chem.* **282,** 5256–5262
8. Tatsumi, K., Sou, Y. S., Tada, N., Nakamura, E., Iemura, S., Natsume, T., Kang, S. H., Chung, C. H., Kasahara, M., Kominami, E., Yamamoto, M., Tanaka, K., and Komatsu, M. (2010) A novel type of E3 ligase for the Ufm1 conjugation system. *J. Biol. Chem.* **285,** 5417–5427
9. Lemaire, K., Moura, R. F., Granvik, M., Igoillo-Esteve, M., Hohmeier, H. E., Hendrickx, N., Newgard, C. B., Waelkens, E., Cnop, M., and Schuit, F. (2011) Ubiquitin fold modifier 1 (UFM1) and its target UFBP1 protect pancreatic $\beta$ cells from ER stress-induced apoptosis. *PLoS One* **6,** e18517
10. Neziri, D., Ilhan, A., Maj, M., Majdic, O., Baumgartner-Parzer, S., Cohen, G., Base, W., and Wagner, L. (2010) Cloning and molecular characterization of Dashurin encoded by C20orf116, a PCI-domain containing protein. *Biochim. Biophys. Acta* **1800,** 430–438
11. Wu, J., Lei, G., Mei, M., Tang, Y., and Li, H. (2010) A novel C53/LZAP-interacting protein regulates stability of C53/LZAP and DDRGK domain-containing Protein 1 (DDRGK1) and modulates NF-$\kappa$B signaling. *J. Biol. Chem.* **285,** 15126–15136
12. Azfer, A., Niu, J., Rogers, L. M., Adamski, F. M., and Kolattukudy, P. E. (2006) Activation of endoplasmic reticulum stress response during the development of ischemic heart disease. *Am. J. Physiol. Heart Circ Physiol* **291,** H1411–1420
13. Lu, H., Yang, Y., Allister, E. M., Wijesekara, N., and Wheeler, M. B. (2008) The identification of potential factors associated with the development of type 2 diabetes: a quantitative proteomics approach. *Mol. Cell Proteomics* **7,** 1434–1451
14. Ha, B. H., Jeon, Y. J., Shin, S. C., Tatsumi, K., Komatsu, M., Tanaka, K., Watson, C. M., Wallis, G., Chung, C. H., and Kim, E. E. (2011) Structure of ubiquitin-fold modifier 1-specific protease UfSP2. *J. Biol. Chem.* **286,** 10248–10257
15. Rasheva, V. I., and Domingos, P. M. (2009) Cellular responses to endoplasmic reticulum stress and apoptosis. *Apoptosis* **14,** 996–1007
16. Wu, J., and Kaufman, R. J. (2006) From acute ER stress to physiological roles of the Unfolded Protein Response. *Cell Death Differ* **13,** 374–384
17. Zhang, Y., Zhang, M., Wu, J., Lei, G., and Li, H. (2012) Transcriptional regulation of the Ufm1 conjugation system in response to disturbance of the endoplasmic reticulum homeostasis and inhibition of vesicle trafficking. *PLoS One* **7,** e48587
18. Brenner, S. (1974) The genetics of *Caenorhabditis elegans*. *Genetics* **77,** 71–94
19. Lewis, J. A., and Fleming, J. T. (1995) Basic culture methods. *Methods Cell Biol.* **48,** 3–29
20. Granato, M., Schnabel, H., and Schnabel, R. (1994) pha-1, a selectable marker for gene transfer in *C. elegans*. *Nucleic Acids Res.* **22,** 1762–1763
21. Studier, F. W. (2005) Protein production by auto-induction in high density shaking cultures. *Protein Expr. Purif.* **41,** 207–234
22. Einarson, M. B., Pugacheva, E. N., and Orlinick, J. R. (2007) Identification of protein-protein interactions with glutathione-S-transferase (GST) fusion proteins. *CSH Protoc.* **2007,** pdb.top11
23. Chien, C. T., Bartel, P. L., Sternglanz, R., and Fields, S. (1991) The two-hybrid system: a method to identify and clone genes for proteins that interact with a protein of interest. *Proc. Natl. Acad. Sci. U.S.A.* **88,** 9578–9582
24. Cardenas, M. E., Hemenway, C., Muir, R. S., Ye, R., Fiorentino, D., and Heitman, J. (1994) Immunophilins interact with calcineurin in the absence of exogenous immunosuppressive ligands. *EMBO J.* **13,** 5944–5957
25. Kim, S. S., Choi, Y. M., and Suh, Y. H. (1997) Lack of interactions between amyloid precursor protein and hydrophilic domains of presenilin 1 and 2

using the yeast two hybrid system. *J. Mol. Neurosci.* **9,** 49–54
26. Shi, J., Kim, K. N., Ritz, O., Albrecht, V., Gupta, R., Harter, K., Luan, S., and Kudla, J. (1999) Novel protein kinases associated with calcineurin B-like calcium sensors in Arabidopsis. *Plant Cell* **11,** 2393–2405
27. Blanchard, D., Hutter, H., Fleenor, J., and Fire, A. (2006) A differential cytolocalization assay for analysis of macromolecular assemblies in the eukaryotic cytoplasm. *Mol. Cell Proteomics* **5,** 2175–2184
28. Schulenburg, H., and Müller, S. (2004) Natural variation in the response of *Caenorhabditis elegans* towards *Bacillus thuringiensis*. *Parasitology* **128,** 433–443
29. Kamath, R. S., and Ahringer, J. (2003) Genome-wide RNAi screening in *Caenorhabditis elegans*. *Methods* **30,** 313–321
30. Bacik, J. P., Walker, J. R., Ali, M., Schimmer, A. D., and Dhe-Paganon, S. (2010) Crystal structure of the human ubiquitin-activating enzyme 5 (UBA5) bound to ATP: mechanistic insights into a minimalistic E1 enzyme. *J. Biol. Chem.* **285,** 20273–20280
31. Mizushima, T., Tatsumi, K., Ozaki, Y., Kawakami, T., Suzuki, A., Ogasahara, K., Komatsu, M., Kominami, E., Tanaka, K., and Yamane, T. (2007) Crystal structure of Ufc1, the Ufm1-conjugating enzyme. *Biochem. Biophys. Res. Commun.* **362,** 1079–1084
32. Ewing, R. M., Chu, P., Elisma, F., Li, H., Taylor, P., Climie, S., McBroom-Cerajewski, L., Robinson, M. D., O'Connor, L., Li, M., Taylor, R., Dharsee, M., Ho, Y., Heilbut, A., Moore, L., Zhang, S., Ornatsky, O., Bukhman, Y. V., Ethier, M., Sheng, Y., Vasilescu, J., Abu-Farha, M., Lambert, J. P., Duewel, H. S., Stewart, I. I., Kuehl, B., Hogue, K., Colwill, K., Gladwish, K., Muskat, B., Kinach, R., Adams, S. L., Moran, M. F., Morin, G. B., Topaloglou, T., and Figeys, D. (2007) Large-scale mapping of human protein-protein interactions by mass spectrometry. *Mol. Syst Biol.* **3,** 89
33. Kwon, J., Cho, H. J., Han, S. H., No, J. G., Kwon, J. Y., and Kim, H. (2010) A novel LZAP-binding protein, NLBP, inhibits cell invasion. *J. Biol. Chem.* **285,** 12232–12240
34. Li, S., Armstrong, C. M., Bertin, N., Ge, H., Milstein, S., Boxem, M., Vidalain, P. O., Han, J. D., Chesneau, A., Hao, T., Goldberg, D. S., Li, N., Martinez, M., Rual, J. F., Lamesch, P., Xu, L., Tewari, M., Wong, S. L., Zhang, L. V., Berriz, G. F., Jacotot, L., Vaglio, P., Reboul, J., Hirozane-Kishikawa, T., Li, Q., Gabel, H. W., Elewa, A., Baumgartner, B., Rose, D. J., Yu, H., Bosak, S., Sequerra, R., Fraser, A., Mango, S. E., Saxton, W. M., Strome, S., Van Den Heuvel, S., Piano, F., Vandenhaute, J., Sardet, C., Gerstein, M., Doucette-Stamm, L., Gunsalus, K. C., Harper, J. W., Cusick, M. E., Roth, F. P., Hill, D. E., and Vidal, M. (2004) A map of the interactome network of the metazoan *C. elegans*. *Science* **303,** 540–543
35. Urano, F., Calfon, M., Yoneda, T., Yun, C., Kiraly, M., Clark, S. G., and Ron, D. (2002) A survival pathway for *Caenorhabditis elegans* with a blocked unfolded protein response. *J. Cell Biol.* **158,** 639–646
36. Corsi, A. K. (2006) A biochemist's guide to *Caenorhabditis elegans*. *Anal. Biochem.* **359,** 1–17
37. Roby, P., Eyre, S., Worthington, J., Ramesar, R., Cilliers, H., Beighton, P., Grant, M., and Wallis, G. (1999) Autosomal dominant (Beukes) premature degenerative osteoarthropathy of the hip joint maps to an 11-cM region on chromosome 4q35. *Am. J. Hum. Genet.* **64,** 904–908
38. Schaefer, H., and Rongo, C. (2006) KEL-8 is a substrate receptor for CUL3-dependent ubiquitin ligase that regulates synaptic glutamate receptor turnover. *Mol. Biol. Cell* **17,** 1250–1260
39. Nam, S., Min, K., Hwang, H., Lee, H. O., Lee, J. H., Yoon, J., Lee, H., Park, S., and Lee, J. (2009) Control of rapsyn stability by the CUL-3-containing E3 ligase complex. *J. Biol. Chem.* **284,** 8195–8206
40. Cui, Y., McBride, S. J., Boyd, W. A., Alper, S., and Freedman, J. H. (2007) Toxicogenomic analysis of *Caenorhabditis elegans* reveals novel genes and pathways involved in the resistance to cadmium toxicity. *Genome Biol.* **8,** R122
41. Ralser, M., Wamelink, M. M., Kowald, A., Gerisch, B., Heeren, G., Struys, E. A., Klipp, E., Jakobs, C., Breitenbach, M., Lehrach, H., and Krobitsch, S. (2007) Dynamic rerouting of the carbohydrate flux is key to counteracting oxidative stress. *J. Biol.* **6,** 10
42. Mori, K. (2009) Signalling pathways in the unfolded protein response: development from yeast to mammals. *J. Biochem.* **146,** 743–750
43. Richardson, C. E., Kinkel, S., and Kim, D. H. (2011) Physiological IRE-1-XBP-1 and PEK-1 signaling in *Caenorhabditis elegans* larval development and immunity. *PLoS Genet.* **7,** e1002391
44. Tatsumi, K., Yamamoto-Mukai, H., Shimizu, R., Waguri, S., Sou, Y. S., Sakamoto, A., Taya, C., Shitara, H., Hara, T., Chung, C. H., Tanaka, K., Yamamoto, M., and Komatsu, M. (2011) The Ufm1-activating enzyme Uba5 is indispensable for erythroid differentiation in mice. *Nat. Commun.* **2,** 181